Int. J. Heat Mass Transfer. Vol. 18, pp. 719–730. Pergamon Press 1975. Printed in Great Britain

IMPINGEMENT COOLING FROM A CIRCULAR JET IN A CROSS FLOW

J.-P. BOUCHEZ
ESA, ESTEC, Noordwijk, The Netherlands

and

R. J. GOLDSTEIN
University of Minnesota, Minneapolis, MN, U.S.A.

(*Received* 5 *February* 1975)

Abstract—Local impingement cooling effectiveness and heat-transfer coefficients are measured over the interaction area of an air jet impinging on a wall and subjected to a cross flow of air. Impingement cooling effectiveness decreases with the blowing rate and at low blowing rates, there is, near the stagnation point, a definite influence of the density ratio. Effectiveness values as high as 60 per cent are obtained at the stagnation point with blowing rate of 12 and nozzle to plate distance of six diameters. The heat-transfer coefficient can be as high as 700 W/(m^2 K) for a blowing rate of twelve with the jet only six diameters above the surface on which it impinges.

NOMENCLATURE

$C_{p\infty}$, specific heat of main stream;
D, diameter of injection tube;
h, heat-transfer coefficient defined using difference between wall and wall recovery temperature or difference between wall and adiabatic wall temperature [see equations (2) and (3)];
h_0, local heat-transfer coefficient without jet flow;
I, momentum flux ratio $\rho_j U_j^2/\rho_\infty U_\infty^2$;
I^*, critical momentum flux ratio above which η becomes independent of density ratio ρ_j/ρ_∞ for a given blowing rate M;
k_∞, thermal conductivity of main stream;
L, distance of jet orifice from wall;
M, blowing rate mass flux ratio/$\rho_j U_j/\rho_\infty U_\infty$;
q, heat flux on wall;
T_j^0, total temperature of jet at jet exit;
T_∞^0, total temperature of main stream before interaction with jet;
T_{aw}, adiabatic wall temperature;
T_w, wall temperature when heat flux is present;
T_r, adiabatic wall temperature when $T_j^0 = T_\infty^0$;
$T_{r'}$, recovery temperature measured on wall without secondary flow ($M = 0$);
U_j, average exit velocity of jet;
U_∞, local velocity of main stream;
U_∞^*, main stream velocity measured at $X/D = -15{\cdot}34$;
X, downstream co-ordinate measured from the centre of the jet orifice;
X''', downstream co-ordinate measured from effective origin of boundary layer;
Z, lateral co-ordinate measured from the centreline of the test section;
η, local effectiveness defined as in equation (1);
μ_∞, dynamic viscosity of main stream;
ρ_j, density of jet at exit;
ρ_∞, density of main stream;

Nu_D, Nusselt number, $Nu_D = \dfrac{hD}{k_\infty}$;

$Re_{X'''}$, Reynolds number, $Re_{X'''} = \dfrac{\rho_\infty U_\infty^* X'''}{\mu_\infty}$;

St, Stanton number, $St = \dfrac{h_0}{\rho_\infty C_{p\infty} U_\infty^*}$.

INTRODUCTION

LOCALIZED cooling of a surface under an intense heat load is of interest in many applications. In one technique to provide such relief, impingement cooling, a two or three dimensional jet is directed toward the regions of high heat input. This process is particularly suited to the protection of local hot spots such as occur near the stagnation region of gas turbine blades. Cooling of other regions of the blade, where the impingement is influenced by the cross flowing coolant from the leading edge, is also of great importance (Fig. 1).

The impingement of circular jets in a quiescent medium has been studied by many investigators. Gauntner, Livingood and Hrycak [1] published a survey on flow characteristics of a single turbulent jet

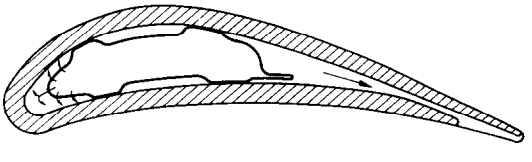

FIG. 1. Impingement cooling in a turbine blade.

impinging on a flat plate. To obtain maximum heat transfer between the jet and the flat plate, it was suggested that the exit of the jet be placed 6·1 diameters above the wall. Hrycak, Lee, Gauntner and Livingood [2] studied the single turbulent jet impinging on a flat plate but this work was restricted to the fluid mechanics aspect of the interaction. Perry [3] looked at the variations of the average heat transfer coefficient when a heated jet impinges on a flat surface at different angles. Nozzle to plate distance was kept constant at 8 diameters and the proposed equation for Nusselt number at the impingement point is similar to relationships used for turbulent flow over a flat plate. Smirnov, Verevochkin and Brdlick [4] studied a submerged liquid jet and only slight modifications were introduced in the results of Perry [3]. Submerged water jets were also investigated by Sitharamayya and Subba Raju [5] but only average values of the Nusselt number were obtained for plates of different diameters. Local values of heat-transfer coefficients were given for axially symmetric jets by Vickers [6] and Gardon and Cobonpue [7], for laminar and turbulent jets respectively. Gardon and Cobonpue [7] found, that the heat transfer coefficient reaches an absolute maximum when the nozzle to plate distance is 6 or 7 diameters. In order to correlate the heat-transfer coefficients corresponding to high jet velocities, the temperature difference used in the definition of the heat-transfer coefficient was the difference between the plate temperature and its recovery temperature measured under similar jet condition. The recovery temperature reached a maximum with a nozzle to plate separation of 11 diameters for Mach numbers between 0·8 and 0·99. Donaldson, Snedeker and Margolis [8, 9] investigated the heat transfer of subsonic symmetric jets impinging perpendicularly on a plate and the influence of turbulence on the heat transfer. The plane two-dimensional jet was studied by Gardon and Akfirat [10] and similar qualitative results were obtained as with the round jet [7]. Jet impingement in a cross flow has to date, received little attention. Colin and Olivari [11] were concerned with the impingement point location, the deepest upstream penetration of the jet, and the size of the jet mixing zone. Tyler and Williamson [12] were similarly interested in the maximum upstream penetration and correlation of the data was given for the upstream stagnation point. Metzger and Korstad [13] reported the effect of cross flow on the heat transfer of an array of jets and results were averaged over a rectangular area of impingement. Kercher and Tabakoff [14] studied the heat-transfer coefficient obtained from a square array of round air jets impinging perpendicularly on a flat surface. There are few numerical solutions. Wolfshtein and Stotter [15] reported numerical solutions for the impingement of a laminar jet when the wall temperature is given as a power function of the radius.

The present work contains the results of an investigation of the flow and heat transfer following perpendicular injection of a circular air jet into a cross flow and the subsequent impingement of the jet on a heated wall.

SOME ANALYTIC CONSIDERATIONS

The temperature distribution on the wall opposite the jet is a function of the location on the wall, the blowing rate M and the density ratio of the jet and main stream fluids [16]. Adiabatic wall temperatures are measured and by extending the suggestion of Gardon and Cobonpue [7] for the heat-transfer coefficient calculation, a wall recovery T_r is used to correlate the data. This is a slight modification to the definition of effectiveness used earlier by Ramsey and Goldstein [17] and Eriksen and Goldstein [18] for film cooling. The impingement cooling effectiveness is defined by

$$\eta = \frac{T_{aw} - T_r}{T_j^0 - T_\infty^0} \tag{1}$$

where T_r is the recovery temperature measured on the adiabatic wall when the total temperature of the jet and main stream are kept equal (i.e. $T_j^0 = T_\infty^0$). T_{aw} and T_r are determined at the same value of M. With a large mainstream velocity the recovery temperature without jet flow ($M = 0$) T_r could be used instead of T_∞^0.

By extending the definition of the heat-transfer coefficient for constant property flow and by using the same difference of temperature as in [7], the heat-transfer coefficient is defined by:

$$h = \frac{q}{T_w - T_{aw}} \tag{2}$$

T_w is the measured temperature on the wall with finite heat flux. T_w and T_{aw} are obtained at the same blowing rate M and total jet temperature T_j^0.

When the total temperature of the jet and main stream are identical, equation (2) reduces to

$$h = \frac{q}{T_w - T_r}. \tag{3}$$

It is found convenient in this work to present the heat-transfer coefficients in a dimensionless form by dividing them by h_0 where h_0 is the heat-transfer coefficient obtained for the same main stream and heat flux conditions but without jet flow ($M = 0$).

If the assumption of a constant property flow is valid, the dimensionless temperature field and impingement cooling effectiveness distributions are the same whether the jet is heated or cooled relative to the main stream. Experimentally, it is simpler to heat the jet and the present results are obtained with density ratio ρ_j/ρ_∞ smaller than unity.

EXPERIMENTAL APPARATUS AND OPERATING CONDITIONS

Air for the wind tunnel is taken from the laboratory room with the flow induced by a "squirrel cage" fan located at the exit of the tunnel. Flow adjustment is provided by a damper, located at the outlet of the blower, forcing a variation in the pressure differential across the fan. Fine adjustment is provided by a sliding band with perforated holes allowing part of the mass flow to by-pass the test section. The boundary-layer flow is rendered turbulent by insertion of a trip upstream of the test plate.

Before entering the contraction section, the flow passes through a straightening section and stainless steel screens. Stagnation temperature and pressure probes are located at the beginning of the test section. Downstream of the test section, a straightening section precedes a divergent section and the fan. A complete description of the experimental apparatus is given in [16]. Figure 2 shows the test section region.

The secondary flow system is supplied by a laboratory compressor delivering air at 8.27 ± 0.07 bar. After filtering, it is regulated to a pressure not exceeding 3·1 bar and the flow is still further controlled by three needle valves in parallel. A stainless steel pipe, 4·09 cm ID, provides a straight section more than 200 cm long to develop the flow before metering it with a stainless steel thin plate orifice. The same pipe contains the flow to the jet orifice and ends with the injection tube which is a straight insulated section 83 cm long. Heating tapes are provided downstream of the thin plate orifice and upstream of the injection tube to raise the temperature of the air jet. When the nozzle to plate distance is 12, the jet orifice is flush with the top wall of the wind tunnel, with a nozzle to plate distance of 6, a splitter plate is used to simulate the inner sleeve of a turbine blade. Figure 3 fully describes the jet configuration for both nozzle to plate distances.

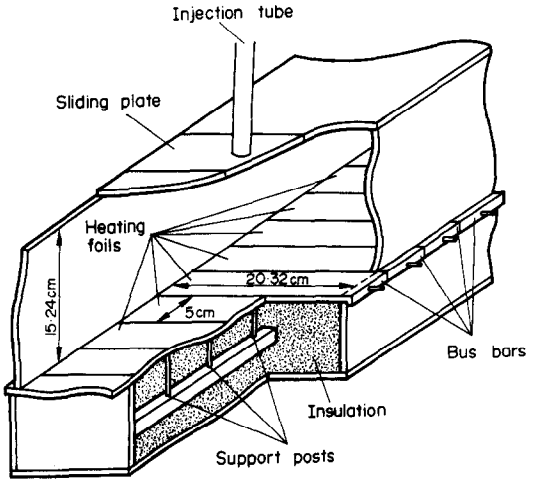

FIG. 2. Test section.

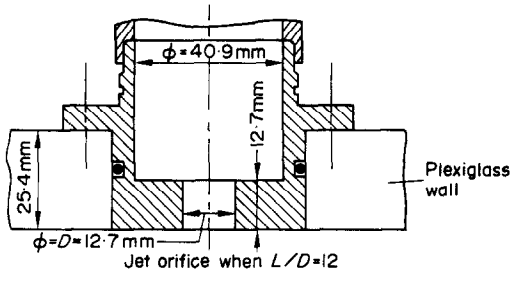

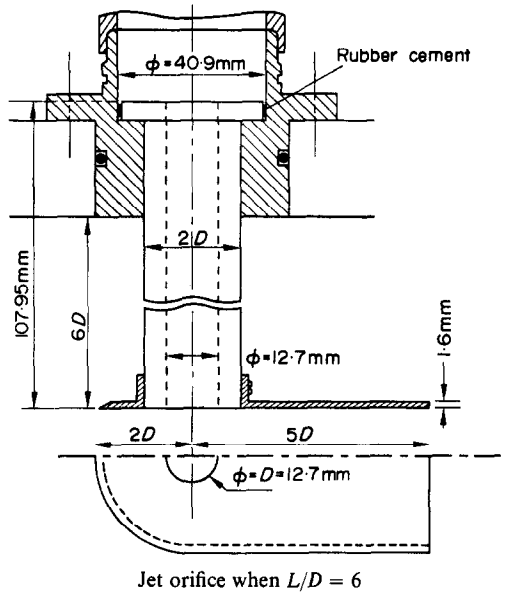

Jet orifice when $L/D = 6$

FIG. 3. Jet orifices.

The test section of the wind tunnel is constructed out of three plexiglass walls and a bottom test plate. The test plate is made of thin Textolite with Styrofoam backing. Stainless steel heaters (25·4 μm thickness) are bonded on the Textolite and 30 gauge iron–constantan thermocouples are imbedded in the test plate in contact with the heaters. Static pressure taps are also drilled through the stainless steel foil. A sliding mechanism is supported on the upper wall of the test section and allows for precise location of either temperature or pressure probes inside the tunnel. Measurements are made to check flow profile, influence of the walls and temperature distribution within the test plate.

Figure 4 gives the heat-transfer results on the test surface without injection and these are used to non-dimensionalize the heat-transfer coefficient corresponding to impingement cooling. The main stream velocity is kept constant during each experiment and its value is fixed at $11{\cdot}96 \pm 0{\cdot}23$ m/s. The jet velocity is widely varied and the blowing rate is adjusted between 12·70 and 3·73.

RESULTS

Flow visualization

Flow visualization is performed using a fog generated by dropping carbon dioxide pellets (dry ice) into a pressure vessel filled with hot water. Pictures are taken for nozzle to plate distances of 6 and 12 diameters and are given in Figs. 5 and 6 respectively. For this part of the experimental program, no splitter plate is used when L/D is 6 as visualization is only intended to give some insight into the flow interaction near the wall. Values given for the blowing rate M are approximate. An outline of the jet interaction in an average sense is given by long time exposure between 1/30 to 1/250 while near instantaneous pictures of the flow are given by the use of a stoboscope of 8 μs illumination.

In Fig. 5, one sees that when the jet impinges violently on the opposite wall, there is a strong turbulent recirculation zone upstream of the impingement area. This vortex is associated with an underpressure readable on the static pressure taps located in the test section floor. Just downstream of this underpressure, an overpressure is present and is in effect the signature of the stagnation point. Due to rapid lateral spreading

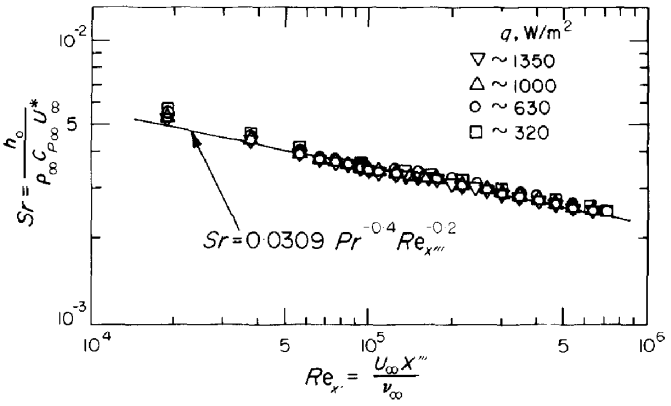

FIG. 4. Heat transfer on test surface (no injection).

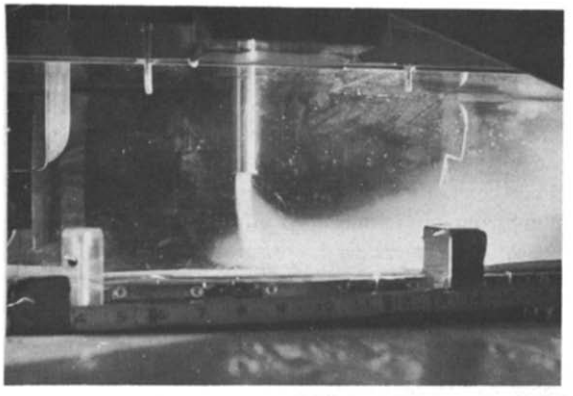

M ≃ 15.5

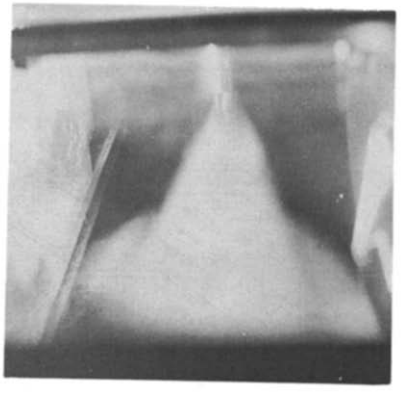

I ≃ 150

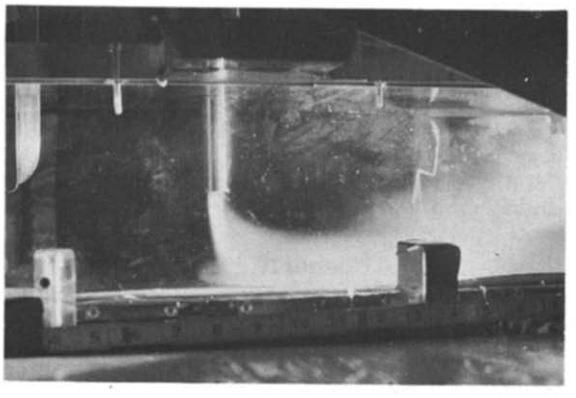

M ≃ 12.5 I ≃ 97

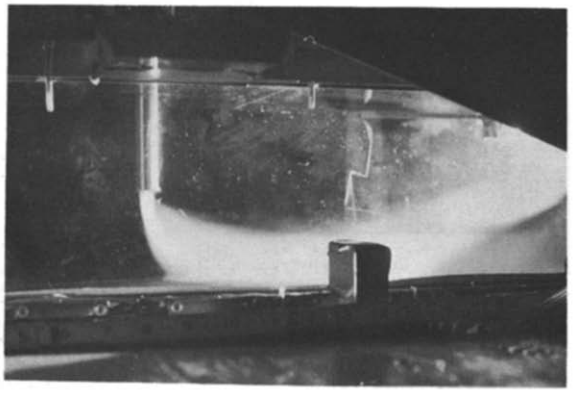

M ≃ 9 I ≃ 50

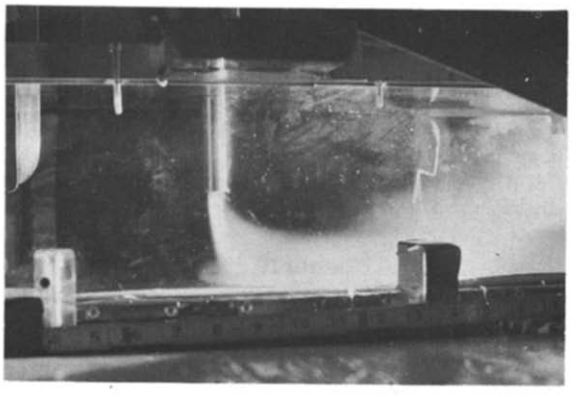

M ≃ 7 I ≃ 31

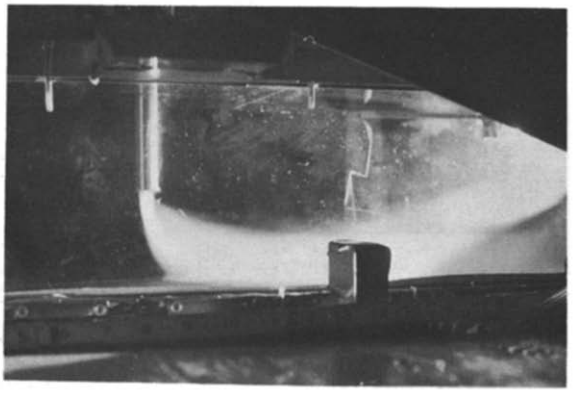

M ≃ 3 I ≃ 6

Shutter speed (1/30–1/250 s)

FIG. 5. Flow visualization ($L/D = 6$).

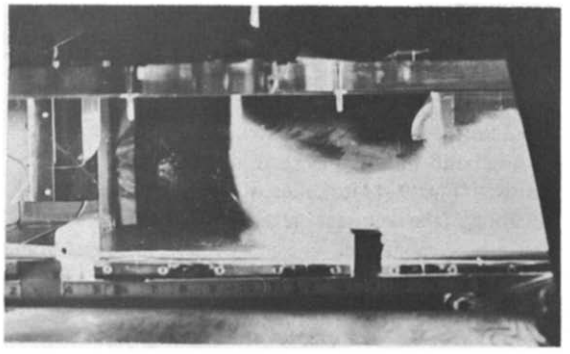

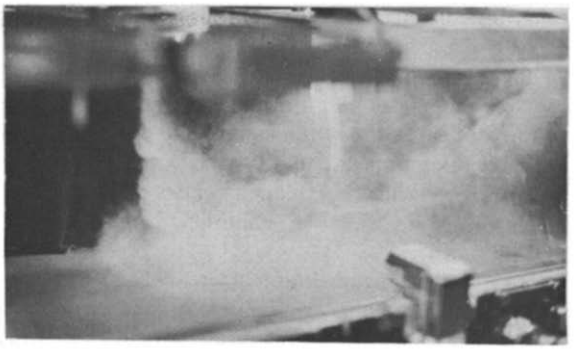

M ≃ 14 I ≃ 123

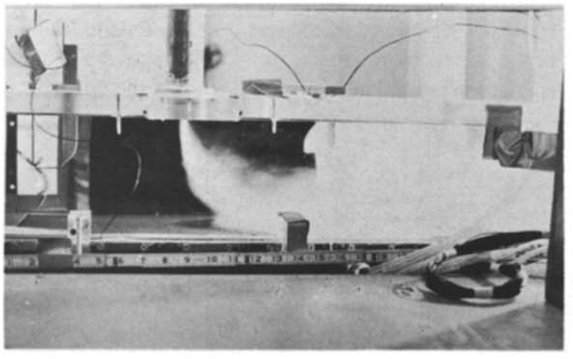

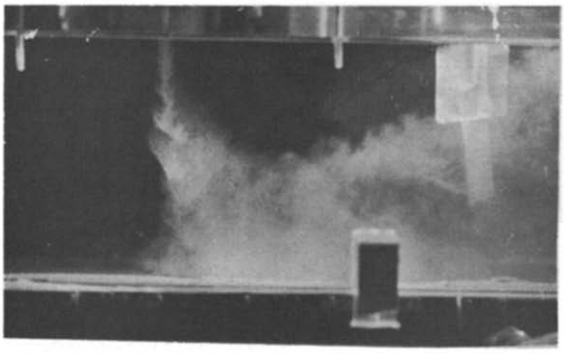

M ≃ 12 I ≃ 90

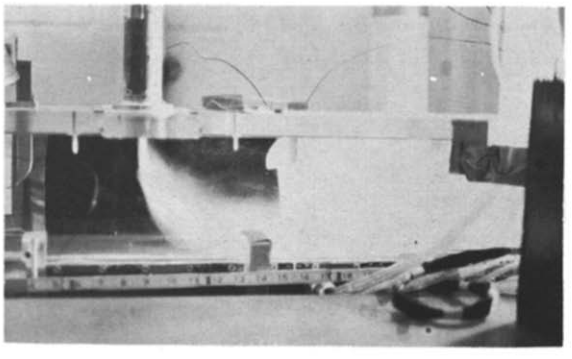

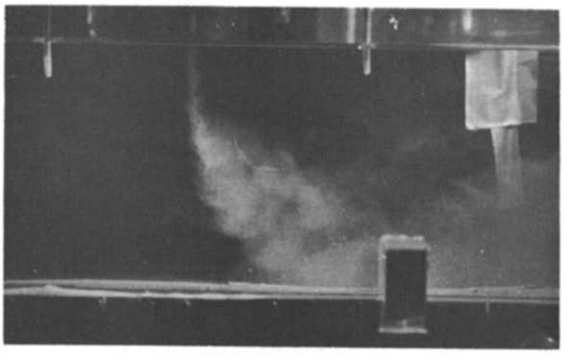

M ≃ 8 I ≃ 40

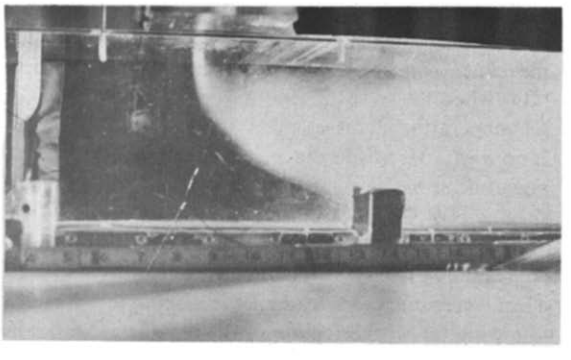

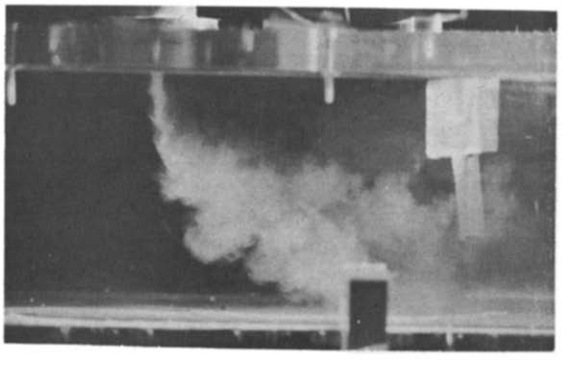

M ≃ 4 I ≃ 10

Shutter speed (1/30-1/250 s) Shutter speed (8 μs)

FIG. 6. Flow visualization (L/D = 12).

of this zone, there is a sidewall effect when the tunnel walls interfere with the flow. This occurs only a few diameters downstream of the stagnation point and causes an uplift of this area of the jet. As the blowing rate decreases, the recirculation zone diminishes and finally disappears as does the underpressure. In Fig. 6, for L/D of 12 the recirculation zone is present at high blowing rate but its importance is somewhat diminished.

From these figures three different regimes are observed at different blowing rates. A recirculation upstream of impingement is associated with high blowing rate. With moderate blowing rates, the recirculation zone disappears but impingement is still present. Finally with low blowing rates, the jet does not have enough momentum to penetrate deep enough into the main stream and there is no impingement on the opposite wall.

[7] for the influence of Mach number on recovery temperature from a circular jet impinging perpendicularly on a plate. The temperature difference is also accentuated in the case of impingement cooling in a cross flow.

Adiabatic wall temperature measurements are presented in Figs. 9–14 for different blowing rates, different location of the secondary jet, and different positions on the impingement wall. The effectiveness increases from zero to a maximum occurring at the stagnation point and uniformly decreases downstream from this point. As the blowing rate decreases, the location of maximum effectiveness is shifted downstream and the maximum value of the effectiveness decreases as expected.

At high blowing rates, the density ratio does not have any significant effect and a characteristic hump in the effectiveness curve is noticeable upstream of the stagnation point. The hump is evidence of the upstream

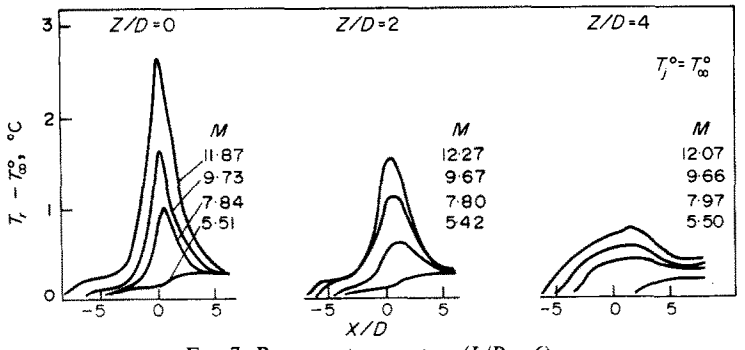

FIG. 7. Recovery temperature ($L/D = 6$).

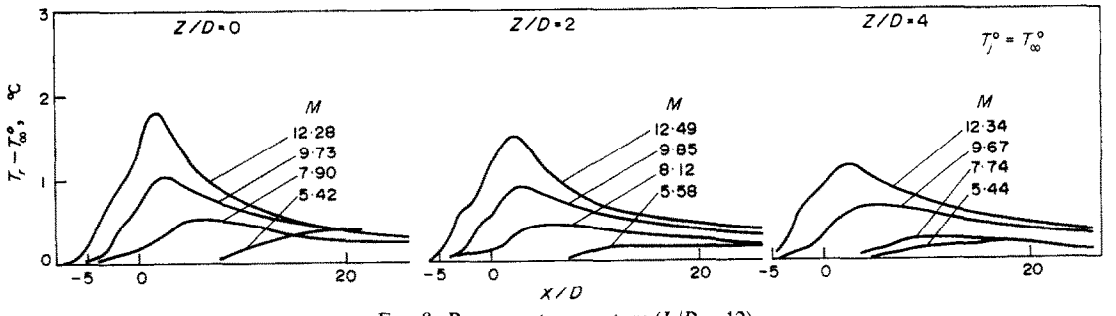

FIG. 8. Recovery temperature ($L/D = 12$).

Impingement cooling effectiveness

In the definition of the effectiveness and heat-transfer coefficient (equations 1 and 3), a wall recovery temperature T_r is defined. T_r is measured when the total temperatures of the jet and main stream are equal and is plotted in Figs. 7 and 8 for the two values of the nozzle to plate spacing. It should be noted that to ignore the value of T_r and to use instead the total main stream temperature T_∞^0 would result in poor correlation and large differences in effectiveness and heat-transfer coefficients near the stagnation region.

In Fig. 7, the difference of temperature between T_r and T_∞^0 corresponding to a blowing rate of 11·87 is approximately 2·65°C. The difference between the two temperatures is appreciable down to a blowing rate of the order of 5·5 which corresponds approximately to a jet Mach number of 0·2. This is somewhat below the minimum value of 0·4 found by Gardon and Cabonpue

recirculation zone and corresponds to a minimum of the stagnation pressure. As the blowing rate decreases, the recirculation zone vanishes as well as the hump and the effectiveness η begins to depend on the density ratio when the blowing rate is kept constant. As the jet temperature increases, that is to say when the density ratio ρ_j/ρ_∞ decreases, the effectiveness increases. This phenomena is shown in Fig. 15 for a nozzle to plate spacing of 6.

At low blowing rate, a decrease in density ratio (at constant M) increases the momentum ratio and the effectiveness increases as the jet is displaced upstream following the weaker action of the cross flow. At high blowing rate, the jet strongly impinges on the opposite surface and although there is an increase of momentum ratio for a decrease in density ratio, there is little upstream motion of the stagnation point as it is already near the jet axis. The adiabatic wall temperature is

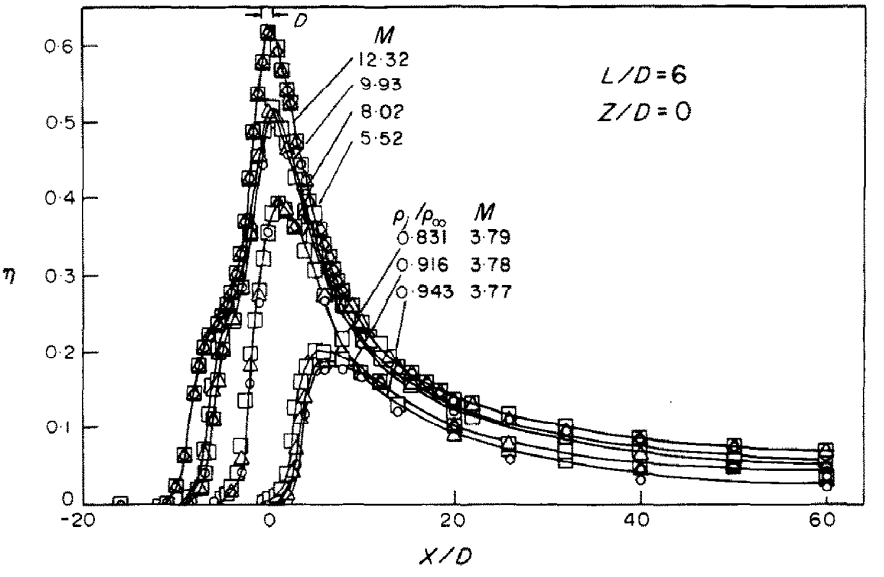

FIG. 9. Downstream effectiveness.

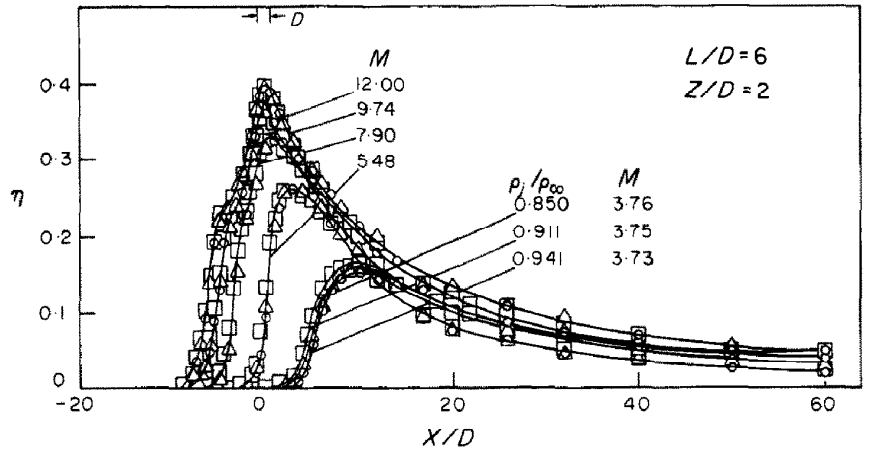

FIG. 10. Downstream effectiveness.

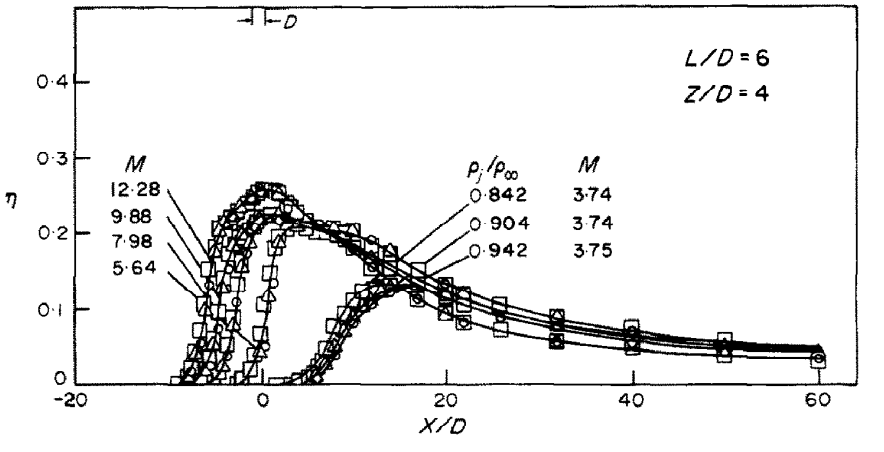

FIG. 11. Downstream effectiveness.

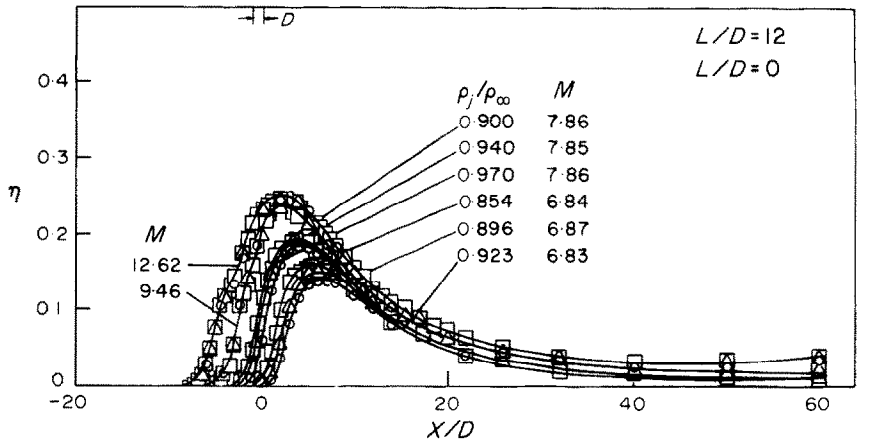

FIG. 12. Downstream effectiveness.

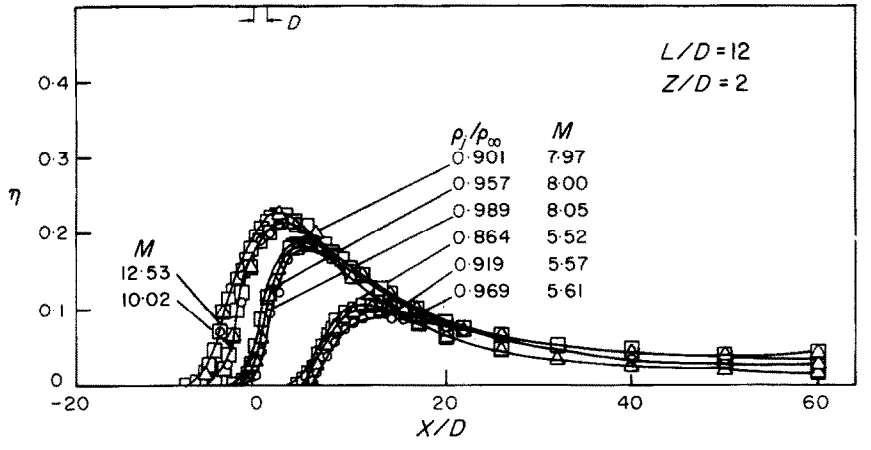

FIG. 13. Downstream effectiveness.

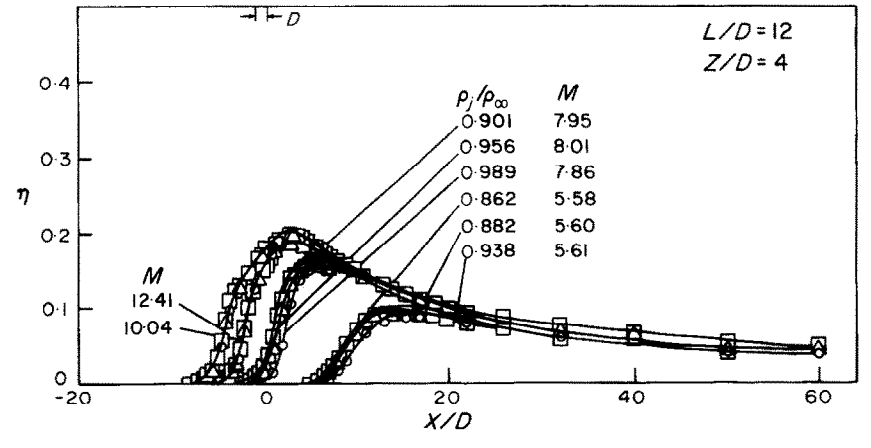

FIG. 14. Downstream effectiveness.

controlled in this case by the inner core of the jet which is nearly constant in location and the value of η remains constant. As the deflection is a function of the momentum ratio, it is suggested that there exists a "critical" value of the momentum ratio I^* above which, the effectiveness is only dependent on the location and the blowing rate M.

From the results presented in Fig. 15, it can be seen that the change occurs between the two lower curves and one can deduce that the value of I^* is in between 17·3 and 31·9 corresponding to the momentum values of one datum on each curve. A similar method leads to the limits of equation (5) when L/D is equal to 12

$$\text{for } L/D = 6 \qquad 17{\cdot}3 < I^* < 31{\cdot}9 \tag{4}$$

$$\text{for } L/D = 12 \qquad 68{\cdot}6 < I^* < 92{\cdot}2. \tag{5}$$

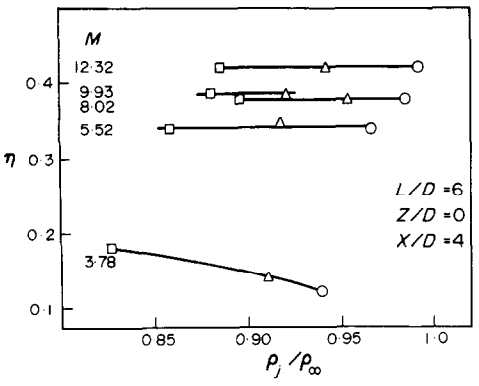

FIG. 15. Variation of effectiveness with density.

The value of I^* does not seem to be a function of the lateral position Z/D but further downstream (larger X/D) the density ratio influence on the local effectiveness diminishes.

Heat-transfer measurements

Heat-transfer results when $T_j^0 = T_\infty^0$ are presented in a normalized form in Figs. 16 and 17 and correspond to the two values of nozzle to plate distances investigated in the study. The use of equation (3) permits the heat-transfer coefficient to be independent of the heat flux which was varied between 300 and 1300 W/m^2. The value of h/h_0 starts at unity far upstream and very slightly decreases upstream of the interaction region.

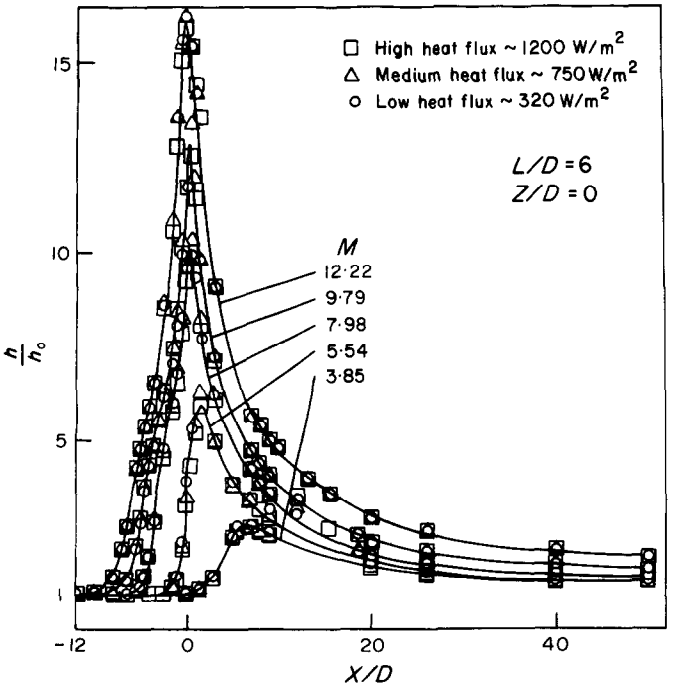

FIG. 16. Heat-transfer coefficient.

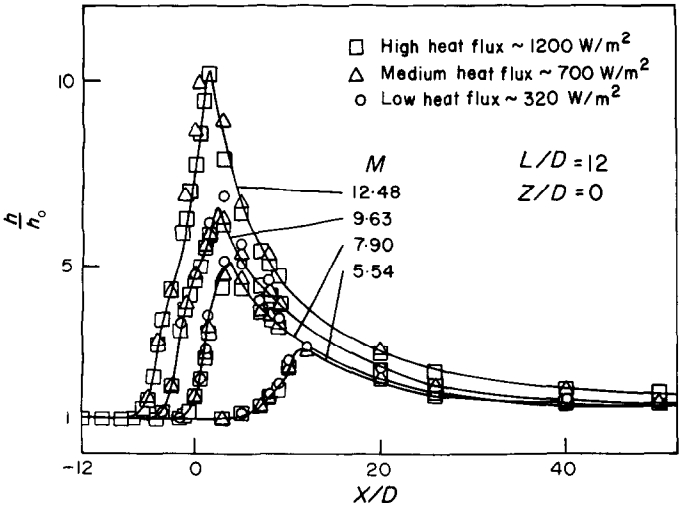

FIG. 17. Heat-transfer coefficient.

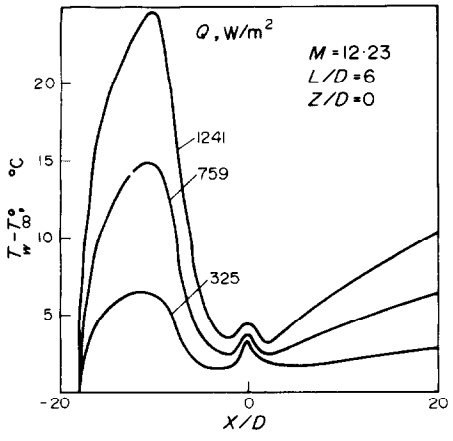

FIG. 18. Temperature distribution along centerline.

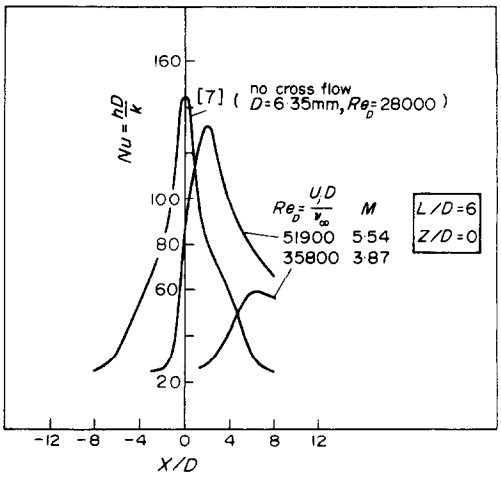

FIG. 19*. Comparison of h along the centerlines.

This is due to a slight decrease in the main stream velocity created by the jet's obstruction of the main flow. The recirculation zone is again indicated by a small hump in the curve. The value of the heat-transfer coefficient increases to its maximum at or near the stagnation point and then decreases monotonically as X/D increases.

The maximum value of the heat transfer does not correspond to the lowest value of wall temperature as is apparent in Fig. 18. The values of the heat-transfer coefficient are very high and values up to 700 W/(m² K) are obtained. To determine the influence of density on the heat-transfer coefficient, tests were run at different densities but constant blowing rate ($M = 8$). No influence of density on the heat-transfer coefficient is found for density ratios between 0·907 and 1·015.

COMPARISON OF RESULTS

The maximum value of the effectiveness was compared to the results of Corrsin and Uberoi [19] for centerline temperature of a non-impinging deflected jet. They define a dimensionless jet centerline temperature which may be compared to η from the present study. For L/D of 6, they predict a dimensionless temperature of 0·66 to 0·80 which can be compared to the maximum value of η of 0·62 at M equal to 12·3 found in the present study. The corresponding numbers at L/D of 12 are 0·32 to 0·39 from [19] and 0·25 at M equal to 12·6 in this present work.

The measured heat-transfer coefficients are compared in Fig. 19 to the work of Gardon and Cobonpue [7]. Results from [7] were obtained without cross flow and it is interesting to note that the Nusselt number with cross flow is lower than in its absence even when the jet Reynolds number is higher. At lower and nearly similar jet Reynolds number, the maximum value of h with cross flow occurs at about 6 diameters downstream and is about 2·5 times smaller than the value obtained without cross flow.

Defining the centerline location by the position at which maximum heat-transfer coefficient occurs, the present results are compared with those of other studies for different values of L/D in Fig. 20. At small L/D in particular, it is difficult to define the exact location of the centerline as thermocouple spacing was $0{\cdot}5D$. Empirical and analytical work of Schetz and Billig [20], Margason [21] and Shandorov [22] have been used for comparison but these values were determined in unbounded space, i.e. without impingement. For small L/D Colin and Olivari [11] found a strong jet is not deflected as much in a bounded space as compared to the same jet in unbounded cross flow; for a weak jet (low M) the effect is reverse. This latter effect is not found in this study with nozzle to plate spacing of 12 diameters.

Comparison of the location of the upstream stagnation point is made with results from Colin and Olivari [11] and Tyler and Williamson [12] and is reported in Fig. 21.

CONCLUSIONS

High jet blowing rates cause a strong interaction at the impingement surface with creation of a recirculation zone upstream of the stagnation point. A moderate blowing rate does not show the recirculation and mixing zone and the stagnation point moves downstream as the jet is deflected by the main stream.

Correlation of the data is achieved using a wall recovery temperature T_r. This temperature is measured on the flat plate when the total temperatures of the jet and main stream are identical, and can be higher than them by a few degrees for high blowing rates. The introduction of this wall recovery temperature renders the effectiveness independent of the density ratio at high blowing rate, while at low blowing rate, effectiveness is a function of both the blowing rate and the density ratio. Values of effectiveness as high as 0·6 and 0·25 are obtained for L/D of 6 and 12 respectively and blowing rates of the order of 12.

Heat-transfer coefficients defined as in equation (3) can be extremely high and values of 700 and 450 W/(m² K) are attained with 6 and 12 diameters nozzle to plate distances respectively at $M = 12$. These

*In Fig. 19, the curve reproduced from the work of Gardon and Cobonpue [7] has not been corrected by the 40 per cent stated by Gardon and Akfirat [10]. By doing so, the Nusselt number without cross flow will decrease and the correlation will be improved.

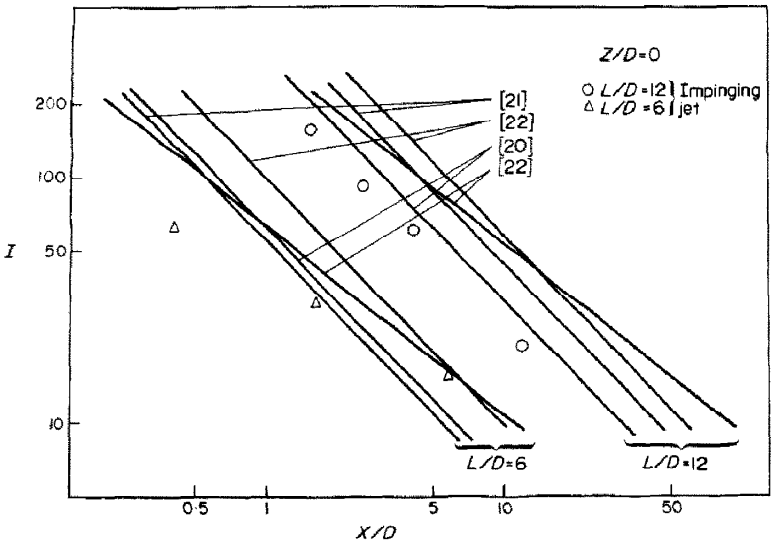

FIG. 20. Location of jet center.

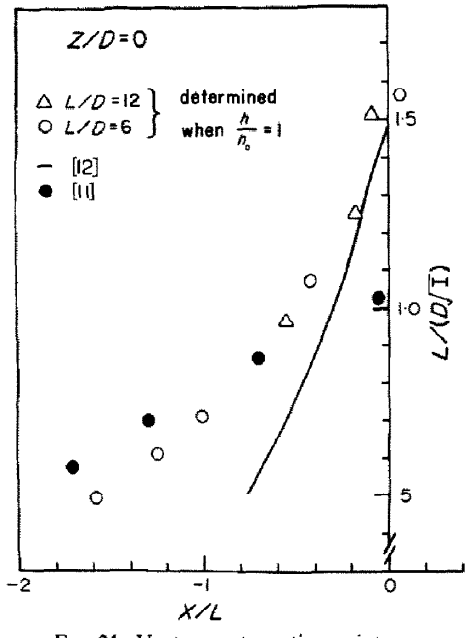

FIG. 21. Upstream stagnation point.

coefficients though much higher than with a turbulent boundary layer on the wall are lower than those reported in the literature for an impinging jet in the absence of cross flow.

Acknowledgements—The work reported herein was conducted at the University of Minnesota Heat Transfer Laboratory with the support of Office of Naval Research under contract N 00014-68-A-0141-0001.

REFERENCES

1. J. W. Gauntner, J. N. B. Livingood and P. Hrycak, Survey of literature on flow characteristics of a single turbulent jet impinging on a flat plate, NASA TN D-5652 (1970).
2. P. Hrycak, D. T. Lee, J. W. Gauntner and J. N. B. Livingood, Experimental flow characteristics of a single turbulent jet impinging on a flat plate, NASA TN D-5690 (1970).
3. K. P. Perry, Heat transfer by convection from a hot gas jet to a plane surface. *Proc. Instn Mech. Engrs* **168**, 775 (1954).
4. V. A. Smirnov, G. E. Verevochkin and P. M. Brdlick, Heat transfer between a jet and a held plate normal to flow, *Int. J. Heat Mass Transfer* **2**, 1 (1961).
5. K. S. R. Sitharamayya, Heat transfer between an axisymmetric jet and a plate held normal to the flow, *Can. J. Chem. Engng* **47**(4), 365 (1969).
6. J. M. F. Vickers, Heat transfer coefficients between fluid jets and normal surfaces, *J. Ind. Engng Chem.* **51**, 967 (1959).
7. R. Gardon and J. Cobonpue, Heat transfer between a flat plate and jets of air impinging on it. *International Development in Heat Transfer, Proceedings, 2nd International Heat Transfer Conference*, p. 454. ASME, New York (1962).
8. C. du P. Donaldson, R. S. Snedeker and D. P. Margolis, A study of free jet impingement, Part 1. Mean properties of free and impinging jets, *J. Fluid Mech.* **45**(2), 281 (1971).
9. C. du P. Donaldson, R. S. Snedeker and D. P. Margolis, A study of free jet impingement, Part 2. Free jet turbulent structures and impingement heat transfer, *J. Fluid Mech.* **45**(3), 477 (1971).
10. R. Gardon and J. C. Akfirat, Heat transfer characteristics of impinging two-dimensional air jets, *J. Heat Transfer* **88C**(1), 101 (1966).
11. P. E. Colin and D. Olivari, The impingement of a circular jet normal to a flat surface with and without cross flow, Von Karman Institute for Fluid Dynamics Technical Report No. 1 (1969).
12. R. A. Tyler and R. G. Williamson, Observations of tunnel flow separation induced by an impinging jet. National Research Council of Canada Report No. NRC 11617 and Aeronautical Report No. LR 537 (1970).
13. D. E. Metzger and R. J. Korstad, Effect of cross flow on impingement heat transfer, *J. Engng Power* **94**, 35 (1972).
14. D. M. Kercher and W. Tabakoff, Heat transfer by a square array of round air jets impinging perpendicular

to a flat surface including the effect of spent air, *J. Engng Power* **92**, 78 (1970).
15. M. Wolfshtein and A. Stotter, Heat transfer between an impinging jet and a flat surface, *Israel J. Technol.* **2**(1), 131 (1964).
16. J.-P. Bouchez, Heat transfer to an impinging circular jet in a cross flow, Ph.D. Thesis, University of Minnesota (1973).
17. J. W. Ramsey and R. J. Goldstein, Interaction of a heated jet with a deflecting stream, *J. Heat Transfer* **83**, 365 (1971).
18. V. L. Eriksen and R. J. Goldstein, Heat transfer and film cooling following normal injection through a round hole, *J. Engng Power* **96**, 329 (1974).
19. S. Corrsin and M. S. Uberoi, Further experiments on the flow and heat transfer in a heated turbulent jet, NASA TR 998 (1950).
20. J. A. Schetz and F. S. Billig, Penetration of gaseous jets injected into a supersonic stream, *J. Spacecraft Rockets* **3**(11), 1658 (1966).
21. R. J. Margason, The path of a jet directed at large angles to a subsonic free stream, NASA TN D-4919 (1968).
22. G. S. Shandorov, Flow from a channel into stationary and moving media, *Zh. Tekh. Fiz.* **37**, 1 (1957).

REFROIDISSEMENT PAR UN JET CIRCULAIRE FRAPPANT UNE PAROI EN PRESENCE D'UN ECOULEMENT TRANSVERSAL

Résumé—L'efficacité du refroidissement local et les coefficients de transfert de chaleur sont mesurés sur la surface d'intéraction d'un jet frappant une paroi en présence d'un écoulement transversal. L'efficacité du refroidissement au contact de la paroi décroit avec la vitesse de soufflage, et pour de faibles vitesses de soufflage le rapport des densités a, près du point d'arrêt, une influence bien déterminée. Des valeurs de l'efficacité aussi élevées que 60 pour cent sont obtenues au point d'arrêt avec des taux de soufflage de 12 et une distance de la paroi à l'embouchure égale à 6 diamètres. Le coefficient de transfert de chaleur peut atteindre une valeur aussi élevée que 700 W/(m^2 °K) pour un taux de soufflage de 12 et un jet situé à 6 diamètres seulement au dessus de la surface qu'il frappe.

AUFPRALLKÜHLUNG DURCH EINEN RUNDEN STRAHL IM KREUZSTROM

Zusammenfassung—Die Kühlwirkung und die örtlichen Wärmeübergangskoeffizienten beim Aufprall eines in einer Querströmung befindlichen Strahls auf eine Wand wurden gemessen. Die Kühlwirkung des Strahls nimmt mit dem Ausblasmengenverhältnis ab; bei kleinen Ausblasmengen ist in der Nähe des Staupunkts ein eindeutiger Einfluß des Dichteverhältnisses festzustellen. Bei einem Ausblasmengenverhältnis von 12 und einem Abstand von Düse zur Wand von 6 Düsendurchmessern werden im Staupunkt Kühlwirkungen bis zu 60% erzielt. In diesem Fall werden Wärmeübergangskoeffizienten bis zu 700 W/m^{2}k erreicht.

ОТВОД ТЕПЛА ОТ КРУГОВОЙ СТРУИ, ПАДАЮЩЕЙ НА ПОВЕРХНОСТЬ, ПРИ НАЛИЧИИ ПОПЕРЕЧНОГО ПОТОКА

Аннотация — Измеряются локальная эффективность охлаждения струи, падающей на поверхность, и коэффициенты теплопереноса в зоне взаимодействия струи и поперечного потока. Эффективность охлаждения уменьшается с уменьшением относительной скорости истечения, и при низких скоростях вблизи критической точки наблюдается определенное влияние отношения плотностей. Величина эффективности в 60% получена в критической точке при скорости относительного истечения, равной 12 и расстоянии между соплом и пластиной, равном 6 диаметрам. Коэффициент теплопереноса может достигать 700 вт(м^2 °К) при относительной скорости истечения, равной 12 и расстоянии над поверхностью, равном 6 диаметрам.